AGU PUBLICATIONS

JGR

Journal of Geophysical Research: Atmospheres

RESEARCH ARTICLE

10.1002/2016JD025359

Key Points:

- The combined effect of urbanization and agriculture on surface temperature was studied in eastern China
- Agriculture offsets surface urban heat island effects with large seasonal and geographic variations
- Evapotranspiration, albedo, and the background climate control the thermal effects associated with urbanization and agriculture

Supporting Information:

- Supporting Information S1

Correspondence to:
D. Zhou,
zhoudc@nuist.edu.cn

Citation:
Zhou, D., D. Li, G. Sun, L. Zhang, Y. Liu, and L. Hao (2016), Contrasting effects of urbanization and agriculture on surface temperature in eastern China, *J. Geophys. Res. Atmos.*, *121*, 9597–9606, doi:10.1002/2016JD025359.

Received 13 MAY 2016
Accepted 8 AUG 2016
Accepted article online 11 AUG 2016
Published online 31 AUG 2016

Contrasting effects of urbanization and agriculture on surface temperature in eastern China

Decheng Zhou[1], Dan Li[2], Ge Sun[3], Liangxia Zhang[1], Yongqiang Liu[4], and Lu Hao[1]

[1]Jiangsu Key Laboratory of Agricultural Meteorology, and College of Applied Meteorology, Nanjing University of Information Science and Technology, Nanjing, China, [2]Department of Earth and Environment, Boston University, Boston, Massachusetts, USA, [3]Eastern Forest Environmental Threat Assessment Center, Southern Research Station, USDA Forest Service, Raleigh, North Carolina, USA, [4]Center for Forest Disturbance Science, Southern Research Station, USDA Forest Service, Athens, Georgia, USA

Abstract The combined effect of urbanization and agriculture, two most pervasive land use activities, on the surface climate remains poorly understood. Using Moderate Resolution Imaging Spectroradiometer data over 2010–2015 and forests as reference, we showed that urbanization warmed the land surface temperature (LST), especially during the daytime and in growing seasons (maximized at 5.0 ± 2.0°C in May), whereas agriculture (dominated by double-cropping system) cooled the LST in two growing seasons during the daytime and all the months but July during the nighttime in Jiangsu Province, eastern China. Collectively, they had insignificant effects on the LST during the day (−0.01°C) and cooled the LST by −0.6°C at night. We also found large geographic variations associated with their thermal effects, indicated by a warming tendency southward. These spatiotemporal patterns depend strongly on vegetation activity, evapotranspiration, surface albedo, and the background climate. Our results emphasize the great potential of agriculture in offsetting the heating effects caused by rapid urbanization in China.

1. Introduction

Humans are altering the Earth's biosphere at an unprecedented rate [*Vitousek et al.*, 1997; *Foley et al.*, 2005; *Grimm et al.*, 2008] through the use of fossil fuels and land use activities [*Kalnay and Cai*, 2003; *Gero et al.*, 2006; *Hossain et al.*, 2012; *Luyssaert et al.*, 2014; *Woldemichael et al.*, 2014]. Over half of natural biomes have been transformed by anthropogenic activities, and further modifications are expected [*Ellis et al.*, 2010; *He et al.*, 2014]. Among these, urbanization and agriculture are the two most pervasive land use activities that can substantially alter the surface climate, particularly temperature, by biogeophysical and biogeochemical effects [*Kalnay and Cai*, 2003; *Pielke et al.*, 2007a, 2007b; *Lei et al.*, 2008; *Georgescu et al.*, 2009a, 2009b; *Kishtawal et al.*, 2010; *Grossman-Clarke et al.*, 2010; *Pielke et al.*, 2011; *Degu et al.*, 2011; *Brovkin et al.*, 2013; *Mahmood et al.*, 2014; *Hao et al.*, 2015].

Urbanization raises the surface temperature by increasing sensible heat flux and ground heat storage at the cost of latent heat flux, resulting in the well-known urban heat island (UHI) effect [*Howard*, 1833; *Oke*, 1982; *Arnfield*, 2003]. The UHI effect has been observed globally except in few arid cities via meteorological stations [*Chow and Roth*, 2006; *Fast et al.*, 2005; *Peterson*, 2003] and thermal infrared remote sensing techniques [*Jin et al.*, 2005; *Zhang et al.*, 2010; *Imhoff et al.*, 2010; *Peng et al.*, 2012; *Clinton and Gong*, 2013; *Zhao et al.*, 2014; *Zhou et al.*, 2014b, 2015, 2016a]. Although urban areas account for a very small proportion of global land surface today, the associated heating effects have already contributed significantly to local, regional, and perhaps global warming [*Kalnay and Cai*, 2003; *Zhou et al.*, 2004; *Grimm et al.*, 2008].

Agriculture, a more widespread land use activity, also has significant potential for altering the climate [*Lobell et al.*, 2009; *Puma and Cook*, 2010; *Cook et al.*, 2011; *Davin et al.*, 2014], whose effects sometimes even exceed those of greenhouse gases emissions [*Bonan*, 1997; *Mahmood et al.*, 2006; *Kueppers et al.*, 2007; *Lobell and Bonfils*, 2008]. On the one hand, the conversion of natural vegetation to crops modifies surface roughness, albedo, leaf conductance, and other properties [*Pielke et al.*, 2007a] and therefore may increase or decrease temperature depending on geographic locations [*Bounoua et al.*, 2002]. On the other hand, land management such as fertilization, no-till agriculture, and double-cropping practice can significantly affect the local climate [*Lobell et al.*, 2006]. Therein, irrigation has perhaps the largest cooling effect on climate [*Kueppers et al.*, 2007; *Lobell and Bonfils*, 2008; *Sacks et al.*, 2009; *Ozdogan et al.*, 2010]. A global modeling study showed that the

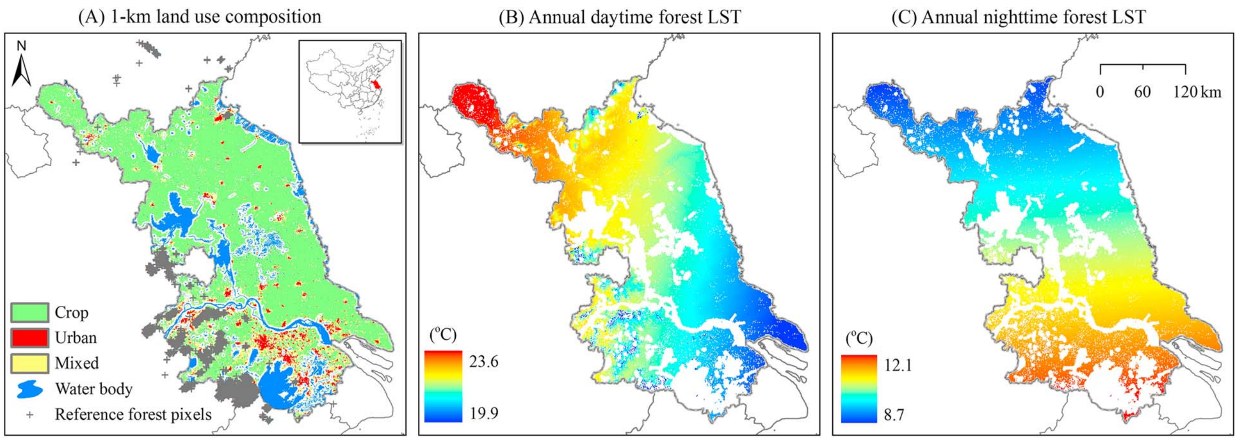

Figure 1. (a) The 1 km urban, crop, and mixed lands and the reference forest pixels derived from 30 m land use map, and (b, c) the annual mean reference land surface temperature (LST) estimated by a simple planar surface model of Jiangsu Province, eastern China. The lands located in the 2 km buffer zones of water body were excluded from this analysis. Albers Conical Equal Area was used as the projection coordinate system.

cooling effect from irrigation is important for all agricultural regions regardless of their climate regimes, with a mean temperature decrease of 1.3°C [*Lobell et al*., 2006].

Although the thermal impacts of urbanization and agriculture have been individually investigated at various spatial and temporal scales, their combined effects on temperature remain largely unknown [*Shi et al*., 2014]. Previous studies indicated that ignoring either would largely underestimate the total impact of land use activities on global warming [*Kalnay and Cai*, 2003; *Shi et al*., 2014]. For example, *Kalnay and Cai* [2003] showed that the surface warming due to land use changes such as urbanization and agriculture from 1950 to 1999 is at least twice as high as the estimates based on urbanization alone in the United States. *Shi et al*. [2014] suggested that the urban warming effect on daily maximum temperature had been canceled by the cooling effect of irrigated croplands in Huang-Huai-Hai Plain of China from 1955 to 2007. Nevertheless, those previous studies mainly focused on the long-term temperature trends rather than the temperature changes relative to natural vegetation. In addition, these studies were based on meteorological observations from a limited number of locations. As a result, a spatially explicit evaluation of the combined impacts of urbanization and agriculture on climate is strongly needed.

This study aims to examine the individual and combined effects of urbanization and agriculture on the LST and explore their driving forces in Jiangsu Province, eastern China. The study region is ideal since it (a) has been experiencing both rapid urbanization and intensive agricultural activities and (b) covers the two major agroclimatic zones (temperate and subtropical) in China. More than 80% of the study region are urbanized or cultivated in 2014 [*Jiangsu Statistics Bureau* (*JSB*), 2015]. The cloud-free Landsat 8 Operational Land Imager (OLI) images are used to characterize land use activities. The Moderate Resolution Imaging Spectroradiometer (MODIS) LST product between 2010 and 2015 is utilized to represent the local thermal environment. LST changes induced by urbanization and agriculture are correlated with a range of biophysical factors to explore the possible causes for their spatial and seasonal variability.

2. Materials and Methods

2.1. Study Area

Jiangsu Province (116°18′–121°57′E, 33°45′–35°20′) is located in eastern China (Figure 1) and has an area of 0.1×10^6 km^2, with 86% plains, lakes and rivers, and 14% low mountains and hills (distributed in the northeast and southwest parts). The climate is characterized by a subtropical humid climate in the southern part and a warm temperate humid climate in the northern part, with the mean annual temperature and precipitation ranging from 13 to 16°C and 800 to 1200 mm, respectively. About three quarters of the land is cultivated for crops or vegetables. The dominant crop type is double-cropping system of rice-wheat/rapeseed in the middle south areas or wheat-maize/soybean in the north part [*JSB*, 2015]. The two growing seasons span from March to May and from July to September, respectively. More than 85% of the cultivated lands are irrigated except for few hill regions [*Siebert et al*., 2013]. Jiangsu Province also experienced rapid urbanization over the past three decades: the urban dwellers increased from only 8.0 million in 1978 to 51.9 million in 2014 [*JSB*, 2015]. There are 13 cities in the province with highly diverse urbanization levels (Figure 1a). The south megalopolis area, including five cities of Nanjing, Zhenjiang, Changzhou, Wuxi, and Suzhou, has nearly half of the total urban population of Jiangsu Province in 2014.

2.2. Land Use Classification

Land use map was derived from the cloud-free Landsat 8 OLI data (downloaded free from http://www.usgs.gov/) with a spatial resolution of 30 m. The land uses were classified into five broad types first (i.e., crop, urban, forest, water body, and unused land), using the Spectral Angle Mapper (SAM) algorithm [*Kruse et al*., 1993]. In order to reduce classification errors caused by similar spectral responses of certain classes such as crop and forest, the land use categories were further refined by using vegetation phenology information [*Xiao et al*., 2006] derived from the Terra MODIS Enhanced Vegetation Index (EVI, 16 day composite) with a spatial resolution of 250 m (MOD13Q1) in 2015. The resulting crop and urban lands account for 72.6% and 10.1% of the total land area, respectively, with the rest being mainly covered by water body (10.1%) and forests (6.7%) (Figure S1 in the supporting information). Further details on land use classification can be found in Text S1 in the supporting information [*Chen et al*., 2004; *Dallimer et al*., 2011; *Foody*, 2002; *Jönsson and Eklundh*, 2004; *Huete et al*., 2002; *Kruse et al*., 1993; *Xiao et al*., 2006; *Zhou et al*., 2014a, 2016b].

In order to match the MODIS LST data (1 km spatial resolution), we calculated the proportions of urban and crop lands for each LST pixel (ρ_{urban} versus ρ_{crop}) and grouped the land uses into three broad types: urban ($\rho_{\text{urban}} > 67\%$), crop ($\rho_{\text{crop}} > 67\%$), and mixed (others). Pixels located in the 2 km buffer zones of water body and those with the sum of ρ_{urban} and ρ_{crop} less than 67% (e.g., dominated by forests) were excluded. About 73,336 pixels (1 km spatial resolution) were included in this analysis, with 83% crop, 4% urban, and 13% mixed (Figure 1a).

2.3. Identifying the Thermal Effects of Urbanization and Agriculture and Their Possible Drivers

In this study, the thermal effects of urbanization and agriculture were defined as the LST differences of urban and crop lands relative to natural forest base condition (ΔT), respectively. LST (has overpass time at 1:30 and 13:30 local solar hours) was obtained from Aqua MODIS 8 days composite products (version 5) with a spatial resolution of 1 km (MYD11A2) from 2010 to 2015. In order to reduce the influences of elevation and geographic locations, a simple planar surface model [e.g., *Anniballe et al*., 2014; *Li et al*., 2015] was first used to estimate the spatially distributed reference temperature (i.e., as a function of longitude, latitude, and altitude) (Figures 1b and 1c). Further details can be found in Text S2 [*Li et al*., 2015; *Jin et al*., 2005; *Tachikawa et al*., 2011; *Wan and Dozier*, 1996; *Wan*, 2008, 2014; *Zhou et al*., 2015; *Wu et al*., 2005]. To investigate the sensitivity of our results to the method of inferring reference temperature, we also quantified the ΔT using two other methods: (a) the reference temperature is estimated as a function of latitude and altitude (i.e., do not consider the longitudinal variations in order to avoid the influence of land sea breeze); and (b) the reference temperature is estimated as the mean of all natural forest pixels (i.e., without including any spatial variability). The reference temperatures estimated using the second method were presented in Figure S2.

Data sets including MODIS EVI, white sky albedo (WSA), and evapotranspiration (ET), and climate parameters (temperature and precipitation) were assembled to examine the possible drivers for ΔT's spatiotemporal variations (Text S3) [*Hijmans et al*., 2005; *Mu et al*., 2011; *Peng et al*., 2012; *Li et al*., 2015]. The EVI, WSA, and ET differences relative to natural forest base conditions (ΔEVI, ΔWSA, and ΔET) were quantified using the same method as that for the ΔT and then were aggregated to monthly levels. The Spearman's correlation coefficients (*r*) between ΔT and these variables across space were calculated for each month. In addition, the *r* between ΔT and those variables across months were calculated on a pixel-by-pixel basis.

3. Results

The area-weighted mean ΔT (2010 to 2015) varied substantially by land use types and seasons in the study region (Figure 2). During the daytime, the urban land was warmer throughout the year (Figure 2a). The ΔT between urban and natural vegetation ranged from 1.0 ± 1.1°C in November to 5.0 ± 2.0°C in May. The mixed land also showed a consistently warming affect, with the magnitude around half of urban land. In contrast, the cropland was cooler in its two growing seasons (March to May and July to September), with

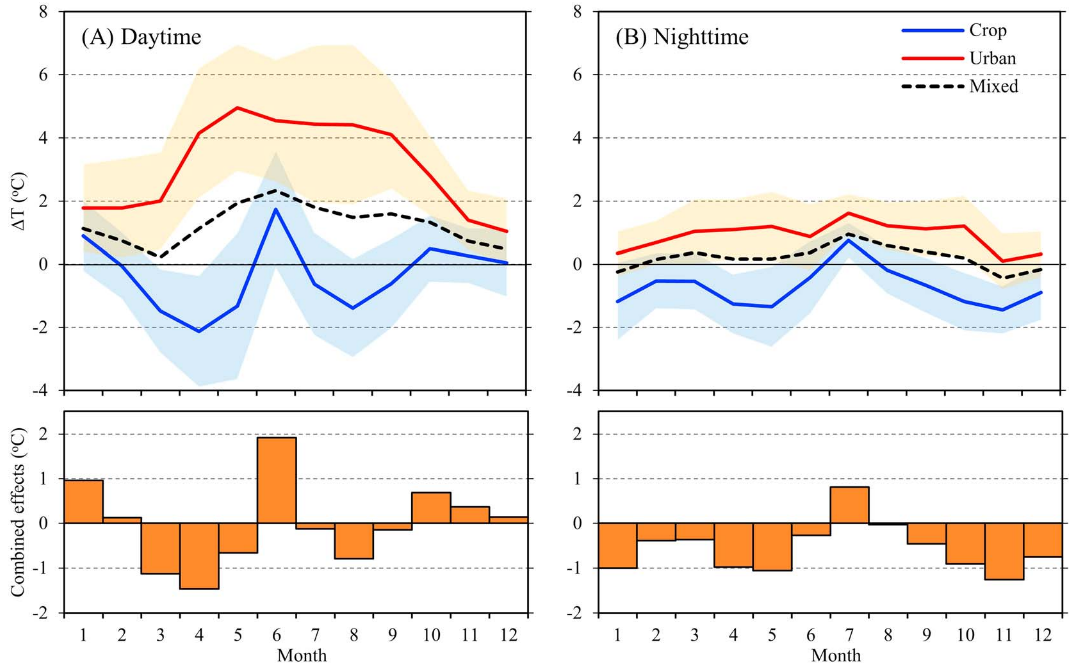

Figure 2. (a, b) Impacts of urban and crop land uses on LST (△*T*) relative to forest base condition and their combined effects in Jiangsu Province, eastern China. The forest LST was calculated as a function of longitude, latitude, and altitude. The shaded area represents 1 standard deviation across space.

the maximum △*T* of −2.1 ± 1.8°C in April. As a result, they together (including urban, crop, and mixed lands) cooled the LST in the two growing seasons (particularly in April by 1.5°C) but warmed the LST in other months and had insignificant effects on the LST (−0.01°C) on an annual mean scale. During the night, the urban land showed a much weaker warming effect, while the cropland continuously cooled the LST in all months except July (Figure 2b). The combination of urban and crop lands reduced nighttime LST by −0.6°C on average. In addition, △T differed across geographic regions (Figure 3). In particular, the cropland had warmer LSTs in the southern part of the study area during the daytime. The urban heat island effects were also higher in the southern regions, especially during the daytime.

Figure 4 shows the correlations between the △*T* estimated by the three methods as described in section 2.3. Spatial distributions of △*T* from the second and third methods can be found in Figures S3 and S4 in the supporting information. As can be seen, the △*T* estimated by the first method that considers variations in latitude, longitude, and altitude was highly consistent with that from the second method that did not consider the longitudinal effects, indicating a small influence of land sea breeze. The third method overestimated the △*T* in the day and underestimated the △*T* at night, and led to a negative △*T* for the majority of urban lands in the nighttime.

To understand the drivers of these spatiotemporal variations, Figure 5 showed the Spearman's correlation coefficients (*r*) between △*T* and five variables across space and months. As can be seen, the intraannual variations of △*T* were closely and negatively correlated with △EVI and △ET in the daytime, with an area-weighted mean *r* of −0.56 and −0.69, respectively, whereas they were more closely and positively related to precipitation (or temperature) at night (Figure 5a). The spatial distributions of △*T* were also negatively correlated ($p < 0.001$) with △EVI and △ET and positively linked to precipitation (or temperature), particularly during the daytime and the two growing seasons (Figure 5b). Additionally, △WSA contributed significantly and negatively to △*T*'s spatial variability in both daytime and nighttime.

4. Discussion

4.1. Contrasting Thermal Effects of Urbanization and Agriculture and Their Drivers

Our results indicated that urbanization led to significant UHI effects. Similar to previous findings [*Imhoff et al.*, 2010; *Peng et al.*, 2012; *Zhou et al.*, 2014b], the UHI effect was clearly larger during the day compared to that at

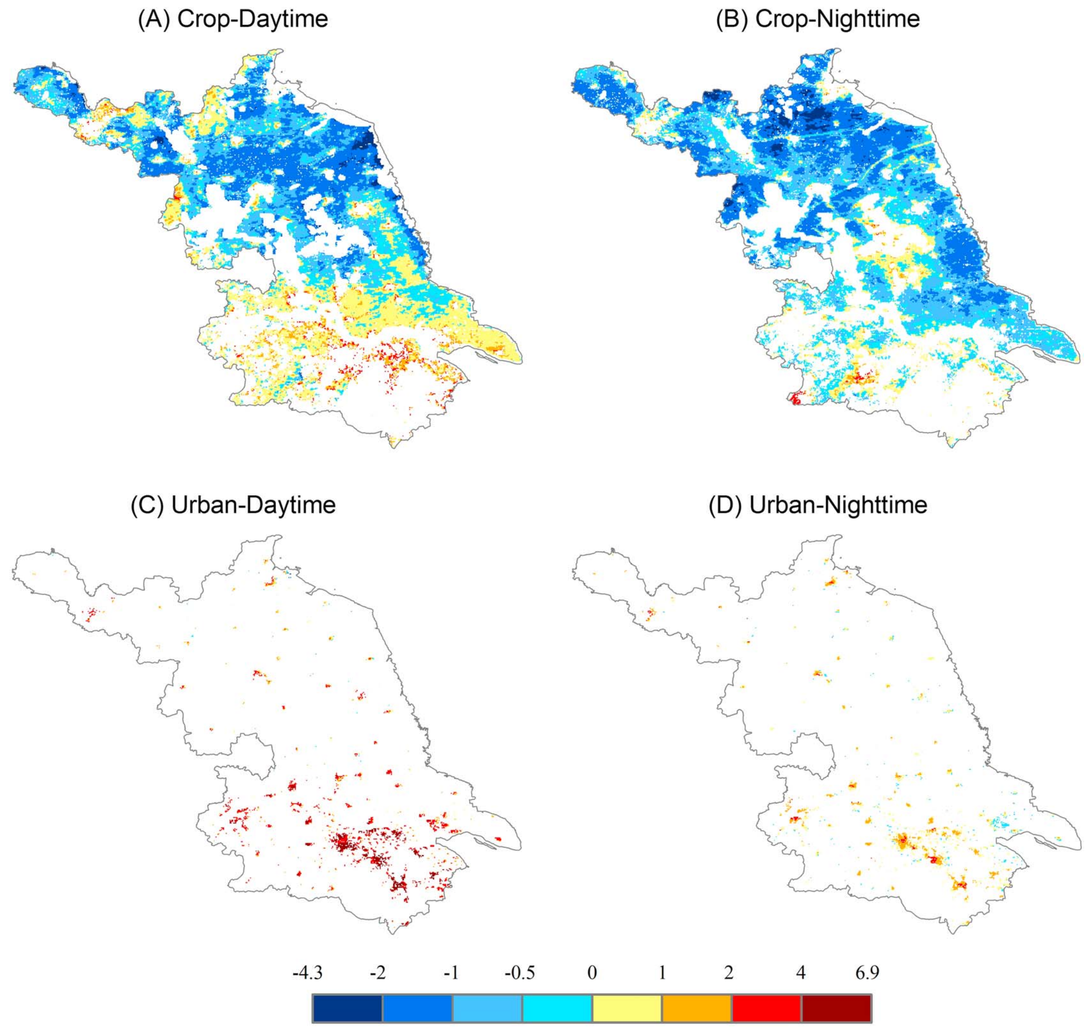

Figure 3. Spatial distributions of the annual mean ΔT (°C) for (a, b) crop and (c, d) urban lands in Jiangsu Province, eastern China. The ΔT of mixed lands were not shown.

night, especially during vegetation growing seasons (April to October) (Figure 2). The stronger daytime UHI effect can be attributed to the substantial decrease of vegetation activity associated with urbanization (Figure 5) [*Zhou et al*., 2014a; *Hao et al*., 2015]. Meanwhile, forests in humid region have high soil moisture content and small surface albedo [*Hall*, 2004; *Zhou et al*., 2016b], which help store heat during the day for later releases, therefore contributing to the relatively smaller nighttime UHI [*Peng et al*., 2012; *Oke*, 1982; *Zhou et al*., 2014b, 2016a].

We found cooling effects of agriculture in the two crop-growing seasons during the daytime (Figure 2), which is consistent with previous studies [*Brovkin et al*., 1999; *Govindasamy et al*., 2001; *Bounoua et al*., 2002; *Matthews et al*., 2004; *Betts et al*., 2007; *Lobell and Bonfils*, 2008; *Fall et al*., 2010]. This phenomenon can be largely explained by the increase of evapotranspiration (i.e., ET) [*Bounoua et al*., 2002; *Lobell and Bonfils*, 2008; *Sacks et al*., 2009], as verified by the strong negative correlations between crop ΔT and ΔET across months (Figure 5). In addition, the higher surface albedo of croplands relative to forests can indirectly exaggerate the cooling impact [*Bounoua et al*., 2002]. Interestingly, the croplands warmed the LST in June, October, and the winter season (Figure 2), possibly due to crop harvesting and the lack of irrigation in those periods.

Moreover, we showed that the croplands continued to cool the LST at night (Figure 2). Similar results have been reported in several previous studies [e.g., *Bonan*, 2001; *Mahmood et al*., 2006; *Kueppers et al*., 2008; *Jin and Miller*, 2011]. The increase in ET and/or the decrease of surface energy input (induced by the increase of surface albedo) during the day not only reduced the sensible heat flux but also decreased the ground heat

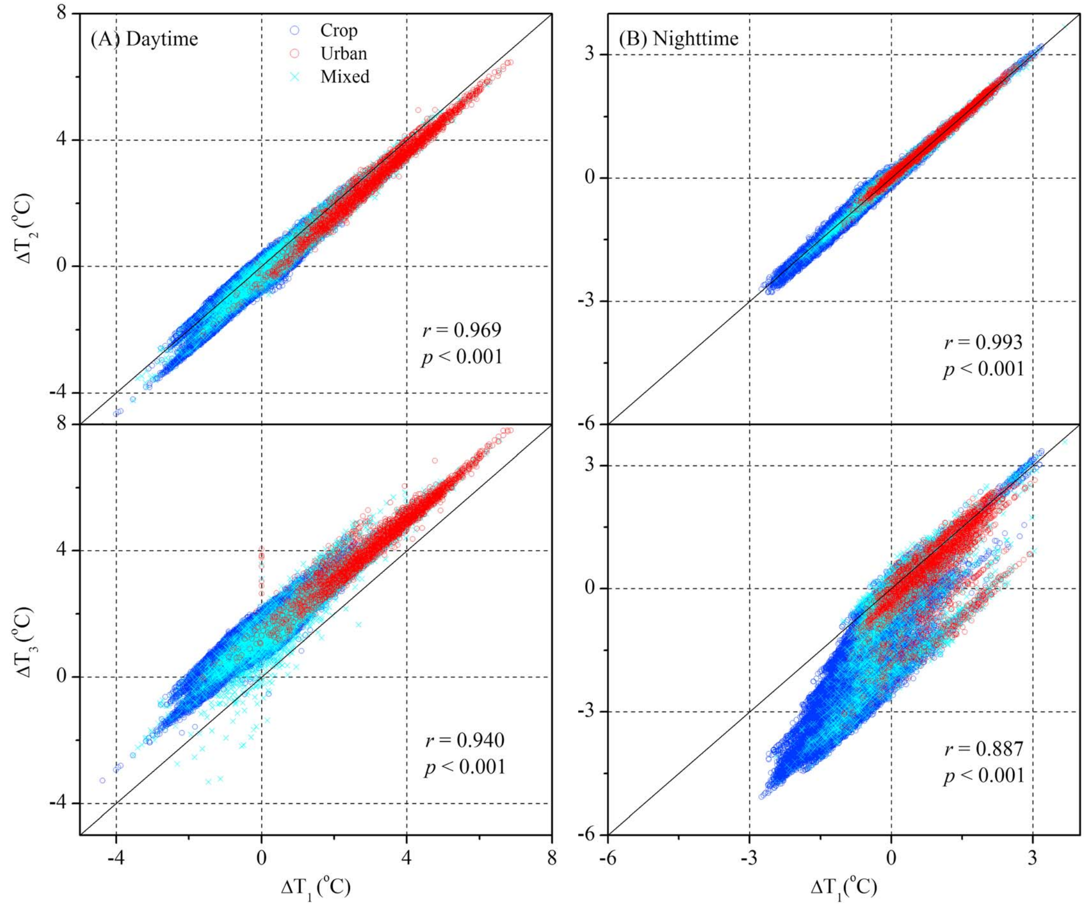

Figure 4. Comparison of annual mean ΔT with reference temperatures obtained from three methods (indicated by the subscript) in Jiangsu Province, eastern China ($N = 73,336$).

storage, therefore might contribute to the cooling effect of croplands at night [*Jin and Miller*, 2011]. Nevertheless, a number of previous studies suggested an insignificant or warming effect of croplands at night due to the irrigation-induced increase in soil heat capacity [*Bounoua et al*., 2002; *Kalnay and Cai*, 2003; *Bonfils and Lobell*, 2007; *Lobell and Bonfils*, 2008; *Shi et al*., 2014]. The reason for the disparity is not clear but might be related to the differences in methods and land surface conditions [e.g., *Bounoua et al*., 2002; *Kueppers* et al., 2008]. For example, most of the previous efforts are based on Regional Climate Models whose results might depend on boundary layer and surface parameterizations [*Kueppers* et al., 2008]. In addition, the thermal infrared LST studied here is usually different from the previously studied air temperature, though they are highly correlated [*Voogt and Oke*, 2003; *Arnfield*, 2003; *Jin and Dickinson*, 2010].

Large spatial variations of ΔT were observed in this study, indicated by a warming effect of cropland in the southern region with a subtropical humid climate (Figure 3). This agrees with some modeling results in other subtropical and tropical regions [*Bounoua et al*., 2002; *Feddema et al*., 2005; *Sampaio et al*., 2007] and can be largely attributed to the reduction of EVI and ET. For example, the subtropical forests typically have large vegetation activity and adequate water for evapotranspiration. Conversion to croplands would reduce the leaf area, rooting depth, and roughness, which decreases the ET [*Sampaio et al*., 2007]. The UHI intensity appeared to be more intensive in the southern region (Figure 3), which can be also attributed to the large urban-induced reduction in EVI [*Zhou et al*., 2014a]. As a result of large spatial variability, urbanization and agriculture overall warmed the LST in the southern region (Figure 3), despite that the spatially averaged effect is small (Figure 2).

4.2. Implications and Uncertainties

We found that the UHI effects can be canceled by the cropland cooling effects in the study region. The cooling effects are expected be more intensive with increasing irrigation extent, crop yields, and cropping density

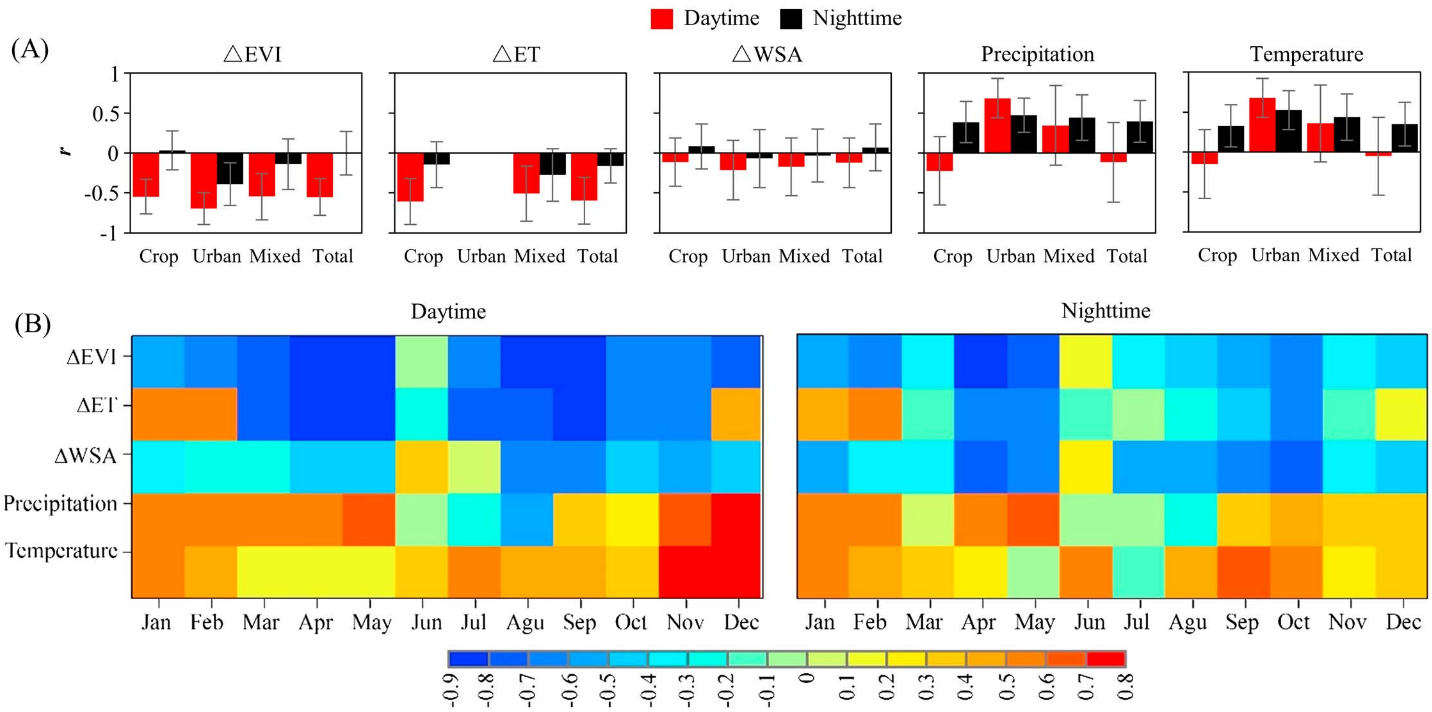

Figure 5. The Spearman's correlation coefficients (*r*) between the △*T* and driving variables (a) across months averaged over different land use compositions, and (b) across space for each month in Jiangsu Province, eastern China. The error bar represents 1 standard deviation. EVI, Enhanced Vegetation Index; ET, Evapotranspiration; WSA, White Sky Albedo; △, difference relative to natural forest base condition. The *r* between urban △*T* and △ET across months was not calculated because there was no ET value for urban land. All the correlations between △*T* and those variables across space were significant at 0.001 levels.

[*Siebert et al*., 2013]. This suggests the necessity of (a) including all land uses (e.g., urbanized and agricultural lands) when evaluating regional climate effects of land use activities, and (b) more studies to guide the reforestation policies (converting croplands to forests) that is often being viewed as one of the strategies to mitigate ongoing global warming [*Peng et al*., 2014]. In addition, we observed evident cooling effects of croplands during the night rather than warming effects previously reveled by some modeling studies [*Bounoua et al*., 2002; *Kalnay and Cai*, 2003; *Bonfils and Lobell*, 2007; *Lobell and Bonfils*, 2008], which may provide important insights for future model improvement. Further, the quantitative methods used in this study (e.g., predicting reference LSTs by using the planar surface model) might also provide new insights for future efforts to evaluate the land use effects on climate.

Uncertainties existed in this analysis. First, we solely focused on the biophysical effects. An additional warming effect is expected if we also consider the greenhouse gases emissions associated with urbanization and agriculture [*Intergovernmental Panel on Climate Change*, 2013]. Second, the reasons for the cooling effects of cropland at night remain elusive. Although it might be related to the increases of latent heat flux and surface albedo which decrease the heat storage, the irrigation-induced increase of soil heat capacity concurrently may increase the heat storage [*Lobell and Bonfils*, 2008]. Third, the croplands are mostly irrigated in the study area but there is no detailed irrigation information for a comparison analysis between irrigated and nonirrigated croplands, which is left for future research. Fourth, the data and technical limitations may introduce uncertainties. For example, around 20% of the time periods have no cloud-free MODIS LST data, especially during the rainiest month of July, which might cause the exceptional warming effect of cropland in July during the night (Figure 2). Worse still, the 8 days MODIS albedo products were invalid in 70% of the total time periods after the data quality control. It also remains challenging to validate the MODIS LST data by in situ measurements due to the lack of free accessible LST in situ data. Note that the MODIS LST data have been widely validated elsewhere, with the absolute bias generally less than 1 K [*Wan*, 2008] and the mean absolute differences relative to in situ measurements less than 5% in urban areas [*Rigo et al*., 2006]. Finally, although we have largely reduced the influence of geographic locations by using the planar surface model, the limited number of natural forest pixels in the northern and eastern (i.e., coastal area) parts of the study region may evoke biases in the fitted reference LST, which might further impact the $\triangle T$. For example, the reference LSTs were overestimated in the coastal areas (i.e., the eastern part) during the daytime by the second method which did not consider the longitudinal effects (cf., Figures 1b and S2a). Nevertheless, the resulting $\triangle T$ was very similar between the two methods (Figure 4), suggesting stronger controls of land surface properties than land sea breeze on $\triangle T$ in the study area.

5. Conclusions

This study focused on the individual and combined effects of urbanization and agriculture on LST in a spatially explicit manner, which serves as the first step toward understanding their contributions to regional climate change. We indicated that there were significant surface urban heat island effects in Jiangsu Province, eastern China, especially during the daytime and summer. In contrast, the croplands cooled the LST, particularly in the two crop-growing seasons (March–May and July–September) during the daytime. Consequently, the urban and crop land uses together had insignificant influences on daytime LST and decreased nighttime LST by −0.6°C with large seasonal variations. We also showed that the thermal effects associated with urbanization and agriculture varied substantially across geographic regions, indicated by a warming effect for both urban and crop lands in the southern part of the study region. These spatiotemporal patterns were found to be closely related to vegetation activity, evapotranspiration, surface albedo, and the background climate. Our results provide new insights to the land use effects on the regional climate and highlight the great potential of agriculture in offsetting the heating effects caused by rapid urbanization in China. However, uncertainties remained in current research, especially regarding the cooling effect of agriculture at night. While remote sensing is cost effective in quantifying land use effects on climate at a regional level, more field observations, numerical modeling, and attribution analyses are required to corroborate the findings from this analysis.

Acknowledgments
The MODIS data are provided by the Land Processes Distributed Active Archive Center (LP DAAC, https://lpdaac.usgs.gov/) managed by the NASA Earth Science Data and Information System (ESDIS) project. The Landsat 8 OLI and DEM data are provided by the U.S. Geological Survey's EROS Data Center (http://eros.usgs.gov/). The climate data are provided by WorldClim, University of California (http://www.worldclim.org/). This study was supported by the Natural Science Foundation of the Jiangsu Higher Education Institutions of China (15KJB170013), the National Natural Science Foundation of China (41501465), and the Startup Foundation for Introducing Talent of NUIST (2014r051). Funding for the visit of the USDA Forest Service is provided by the China Scholarship Council.

References

Anniballe, R., S. Bonafoni, and M. Pichierri (2014), Spatial and temporal trends of the surface and air heat island over Milan using MODIS data, *Remote Sens. Environ.*, *150*, 163–171.
Arnfield, A. J. (2003), Two decades of urban climate research: A review of turbulence, exchanges of energy and water, and the urban heat island, *Int. J. Climatol.*, *23*(1), 1–26.
Betts, R. A. (2001), Biogeophysical impacts of land use on present-day climate: Near-surface temperature change and radiative forcing, *Atmos. Sci. Lett.*, *2*(1–4), 39–51.
Betts, R. A., P. D. Falloon, K. K. Goldewijk, and N. Ramankutty (2007), Biogeophysical effects of land use on climate: Model simulations of radiative forcing and large-scale temperature change, *Agric. For. Meteorol.*, *142*(2), 216–233.
Bonan, G. B. (1997), Effects of land use on the climate of the United States, *Clim. Change*, *37*(3), 449–486.
Bonan, G. B. (2001), Observational evidence for reduction of daily maximum temperature by croplands in the midwest United States, *J. Clim.*, *14*, 2430–2442.
Bonfils, C., and D. Lobell (2007), Empirical evidence for a recent slowdown in irrigation-induced cooling, *Proc. Natl. Acad. Sci. U. S. A.*, *104*(34), 13,582–13,587.
Bounoua, L., R. DeFries, G. J. Collatz, P. Sellers, and H. Khan (2002), Effects of land cover conversion on surface climate, *Clim. Change*, *52*(1–2), 29–64.
Brovkin, V., A. Ganopolski, M. Claussen, C. Kubatzki, and V. Petoukhov (1999), Modelling climate response to historical land cover change, *Glob. Ecol. Biogeogr.*, *8*(6), 509–517.
Brovkin, V., L. Boysen, V. Arora, J. Boisier, P. Cadule, L. Chini, M. Claussen, P. Friedlingstein, V. Gayler, and B. Van Den Hurk (2013), Effect of anthropogenic land-use and land-cover changes on climate and land carbon storage in CMIP5 projections for the twenty-first century, *J. Clim.*, *26*(18), 6859–6881.
Chen, J., P. Jönsson, M. Tamura, Z. Gu, B. Matsushita, and L. Eklundh (2004), A simple method for reconstructing a high-quality NDVI time-series data set based on the Savitzky–Golay filter, *Remote Sens. Environ.*, *91*(3), 332–344.
Chow, W. T. L., and M. Roth (2006), Temporal dynamics of the urban heat island of Singapore, *Int. J. Climatol.*, *26*(15), 2243–2260.
Clinton, N., and P. Gong (2013), MODIS detected surface urban heat islands and sinks: Global locations and controls, *Remote Sens. Environ.*, *134*, 294–304.
Cook, B. I., M. J. Puma, and N. Y. Krakauer (2011), Irrigation induced surface cooling in the context of modern and increased greenhouse gas forcing, *Clim. Dyn.*, *37*(7–8), 1587–1600.
Dallimer, M., Z. Tang, P. R. Bibby, P. Brindley, K. J. Gaston, and Z. G. Davies (2011), Temporal changes in greenspace in a highly urbanized region, *Biol. Lett.*, *7*(5), 763–766.
Davin, E. L., S. I. Seneviratne, P. Ciais, A. Olioso, and T. Wang (2014), Preferential cooling of hot extremes from cropland albedo management, *Proc. Natl. Acad. Sci. U. S. A.*, *111*(27), 9757–9761.
Degu, A. M., F. Hossain, D. Niyogi, R. Pielke, J. M. Shepherd, N. Voisin, and T. Chronis (2011), The influence of large dams on surrounding climate and precipitation patterns, *Geophys. Res. Lett.*, *38*, L04405, doi:10.1029/2010GL046482.
Ellis, E. C., K. Klein Goldewijk, S. Siebert, D. Lightman, and N. Ramankutty (2010), Anthropogenic transformation of the biomes, 1700 to 2000, *Global Ecol. Biogeogr.*, *19*(5), 589–606.
Fall, S., D. Niyogi, A. Gluhovsky, R. A. Pielke, E. Kalnay, and G. Rochon (2010), Impacts of land use land cover on temperature trends over the continental United States: Assessment using the North American Regional Reanalysis, *Int. J. Climatol.*, *30*(13), 1980–1993.

Fast, J. D., J. C. Torcolini, and R. Redman (2005), Pseudovertical temperature profiles and the urban heat island measured by a temperature datalogger network in Phoenix, Arizona, *J. Appl. Meteorol.*, *44*(1), 3–13.
Feddema, J. J., K. W. Oleson, G. B. Bonan, L. O. Mearns, L. E. Buja, G. A. Meehl, and W. M. Washington (2005), The importance of land-cover change in simulating future climates, *Science*, *310*(5754), 1674–1678.
Foley, J. A., R. DeFries, G. P. Asner, C. Barford, G. Bonan, S. R. Carpenter, F. S. Chapin, M. T. Coe, G. C. Daily, and H. K. Gibbs (2005), Global consequences of land use, *Science*, *309*(5734), 570–574.
Foody, G. M. (2002), Status of land cover classification accuracy assessment, *Remote Sens. Environ.*, *80*(1), 185–201.
Georgescu, M., G. Miguez-Macho, L. Steyaert, and C. Weaver (2009a), Climatic effects of 30 years of landscape change over the Greater Phoenix, Arizona, region: 1. Surface energy budget changes, *J. Geophys. Res.*, *114*, D05110, doi:10.1029/2008JD010745.
Georgescu, M., G. Miguez-Macho, L. Steyaert, and C. Weaver (2009b), Climatic effects of 30 years of landscape change over the Greater Phoenix, Arizona, region: 2. Dynamical and thermodynamical response, *J. Geophys. Res.*, *114*, D05111, doi:10.1029/2008JD010762.
Gero, A., A. Pitman, G. Narisma, C. Jacobson, and R. Pielke (2006), The impact of land cover change on storms in the Sydney Basin, Australia, *Global Planet. Change*, *54*(1), 57–78.
Govindasamy, B., P. Duffy, and K. Caldeira (2001), Land use changes and Northern Hemisphere cooling, *Geophys. Res. Lett.*, *28*(2), 291–294, doi:10.1029/2000GL006121.
Grimm, N. B., S. H. Faeth, N. E. Golubiewski, C. L. Redman, J. Wu, X. Bai, and J. M. Briggs (2008), Global change and the ecology of cities, *Science*, *319*(5864), 756–760.
Grossman-Clarke, S., J. A. Zehnder, T. Loridan, and C. S. B. Grimmond (2010), Contribution of land use changes to near-surface air temperatures during recent summer extreme heat events in the Phoenix metropolitan area, *J. Appl. Meteorol. Climatol.*, *49*(8), 1649–1664.
Hall, A. (2004), The role of surface albedo feedback in climate, *J. Clim.*, *17*(7), 1550–1568.
Hao, L., G. Sun, Y. Liu, J. Wan, M. Qin, H. Qian, C. Liu, J. Zheng, R. John, and P. Fan (2015), Urbanization dramatically altered the water balances of a paddy field-dominated basin in southern China, *Hydrol. Earth Syst. Sci.*, *19*(7), 3319–3331.
He, F., S. J. Vavrus, J. E. Kutzbach, W. F. Ruddiman, J. O. Kaplan, and K. M. Krumhardt (2014), Simulating global and local surface temperature changes due to Holocene anthropogenic land cover change, *Geophys. Res. Lett.*, *41*, 623–631, doi:10.1002/2013GL058085.
Hijmans, R. J., S. E. Cameron, J. L. Parra, P. G. Jones, and A. Jarvis (2005), Very high resolution interpolated climate surfaces for global land areas, *Int. J. Climatol.*, *25*(15), 1965–1978.
Hossain, F., A. M. Degu, W. Yigzaw, S. Burian, D. Niyogi, J. M. Shepherd, and R. Pielke Sr. (2012), Climate feedback-based provisions for dam design, operations, and water management in the 21st century, *J. Hydrol. Eng.*, *17*(8), 837–850.
Howard, L. (1833), *Climate of London Deduced from Metrological Observations*, vol. 1, Harvey and Dorton Press, London.
Huete, A., K. Didan, T. Miura, E. P. Rodriguez, X. Gao, and L. G. Ferreira (2002), Overview of the radiometric and biophysical performance of the MODIS vegetation indices, *Remote Sens. Environ.*, *83*(1), 195–213.
Imhoff, M. L., P. Zhang, R. E. Wolfe, and L. Bounoua (2010), Remote sensing of the urban heat island effect across biomes in the continental USA, *Remote Sens. Environ.*, *114*(3), 504–513.
Intergovernmental Panel on Climate Change (2013), *Climate Change 2013: The Physical Science Basis. Contribution of Working Group I to the Fifth Assessment Report of the Intergovernmental Panel on Climate Change*, pp. 1535 , Cambridge Univ. Press, Cambridge, UK and New York, N. Y.
Jiangsu Statistics Bureau (JSB) (2015), Jiangsu Statistical Yearbook 2015. [Available at http://www.jssb.gov.cn/2015nj/indexc.htm.]
Jin, J., and N. L. Miller (2011), Regional simulations to quantify land use change and irrigation impacts on hydroclimate in the California Central Valley, *Theor. Appl. Clim.*, *104*(3–4), 429–442.
Jin, M., and R. E. Dickinson (2010), Land surface skin temperature climatology: Benefitting from the strengths of satellite observations, *Environ. Res. Lett.*, *5*(4, 044004).
Jin, M., R. E. Dickinson, and D. Zhang (2005), The footprint of urban areas on global climate as characterized by MODIS, *J. Clim.*, *18*(10), 1551–1565.
Jönsson, P., and L. Eklundh (2004), TIMESAT—A program for analyzing time-series of satellite sensor data, *Comput. Geosci.*, *30*(8), 833–845.
Kalnay, E., and M. Cai (2003), Impact of urbanization and land-use change on climate, *Nature*, *423*(6939), 528–531.
Kishtawal, C. M., D. Niyogi, M. Tewari, R. A. Pielke, and J. M. Shepherd (2010), Urbanization signature in the observed heavy rainfall climatology over India, *Int. J. Climatol.*, *30*(13), 1908–1916.
Kruse, F., A. Lefkoff, J. Boardman, K. Heidebrecht, A. Shapiro, P. Barloon, and A. Goetz (1993), The spectral image processing system (SIPS)—Interactive visualization and analysis of imaging spectrometer data, *Remote Sens. Environ.*, *44*(2), 145–163.
Kueppers, L. M., M. A. Snyder, and L. C. Sloan (2007), Irrigation cooling effect: Regional climate forcing by land-use change, *Geophys. Res. Lett.*, *34*, L03703, doi:10.1029/2006GL028679.
Kueppers, L. M., et al. (2008), Seasonal temperature responses to land-use change in the western United States, Global Planet. *Change*, *60*(3–4), 250–264
Lei, M., D. Niyogi, C. Kishtawal, R. Pielke Sr., A. Beltrán-Przekurat, T. Nobis, and S. Vaidya (2008), Effect of explicit urban land surface representation on the simulation of the 26 July 2005 heavy rain event over Mumbai, India, *Atmos. Chem. Phys.*, *8*(20), 5975–5995.
Li, Y., M. Zhao, S. Motesharrei, Q. Mu, E. Kalnay, and S. Li (2015), Local cooling and warming effects of forests based on satellite observations, *Nat. Commun.*, *6*.
Lobell, D. B., and C. Bonfils (2008), The effect of irrigation on regional temperatures: A spatial and temporal analysis of trends in California, 1934–2002, *J. Clim.*, *21*(10), 2063–2071.
Lobell, D., G. Bala, and P. Duffy (2006), Biogeophysical impacts of cropland management changes on climate, *Geophys. Res. Lett.*, *33*, L06708, doi:10.1029/2005GL025492.
Lobell, D., G. Bala, A. Mirin, T. Phillips, R. Maxwell, and D. Rotman (2009), Regional differences in the influence of irrigation on climate, *J. Clim.*, *22*(8), 2248–2255.
Luyssaert, S., M. Jammet, P. C. Stoy, S. Estel, J. Pongratz, E. Ceschia, G. Churkina, A. Don, K. Erb, and M. Ferlicoq (2014), Land management and land-cover change have impacts of similar magnitude on surface temperature, *Nat. Clim. Change*, *4*(5), 389–393.
Mahmood, R., S. A. Foster, T. Keeling, K. G. Hubbard, C. Carlson, and R. Leeper (2006), Impacts of irrigation on 20th century temperature in the northern Great Plains, *Global Planet. Change*, *54*(1), 1–18.
Mahmood, R., R. A. Pielke, K. G. Hubbard, D. Niyogi, P. A. Dirmeyer, C. McAlpine, A. M. Carleton, R. Hale, S. Gameda, and A. Beltrán-Przekurat (2014), Land cover changes and their biogeophysical effects on climate, *Int. J. Climatol.*, *34*(4), 929–953.
Matthews, H., A. Weaver, K. Meissner, N. Gillett, and M. Eby (2004), Natural and anthropogenic climate change: Incorporating historical land cover change, vegetation dynamics and the global carbon cycle, *Clim. Dyn.*, *22*(5), 461–479.
Mu, Q., M. Zhao, and S. W. Running (2011), Improvements to a MODIS global terrestrial evapotranspiration algorithm, *Remote Sens. Environ.*, *115*(8), 1781–1800.
Oke, T. R. (1982), The energetic basis of the urban heat island, *Q. J. R. Meteorol. Soc.*, *108*(455), 1–24.

Ozdogan, M., M. Rodell, H. K. Beaudoing, and D. L. Toll (2010), Simulating the effects of irrigation over the United States in a land surface model based on satellite-derived agricultural data, *J. Hydrometeorol.*, *11*(1), 171–184.

Peng, S. S., S. Piao, Z. Zeng, P. Ciais, L. Zhou, L. Z. Li, R. B. Myneni, Y. Yin, and H. Zeng (2014), Afforestation in China cools local land surface temperature, *Proc. Natl. Acad. Sci. U. S. A.*, *111*(8), 2915–2919.

Peng, S., S. Piao, P. Ciais, P. Friedlingstein, C. Ottle, F. M. Bréon, H. Nan, L. Zhou, and R. B. Myneni (2012), Surface urban heat island across 419 global big cities, *Environ. Sci. Technol.*, *46*(2), 696–703.

Peterson, T. C. (2003), Assessment of urban versus rural in situ surface temperatures in the contiguous United States: No difference found, *J. Clim.*, *16*(18), 2941–2959.

Pielke, R. A., J. O. Adegoke, T. N. Chase, C. H. Marshall, T. Matsui, and D. Niyogi (2007a), A new paradigm for assessing the role of agriculture in the climate system and in climate change, *Agric. For. Meteorol.*, *142*(2), 234–254.

Pielke, R. A., J. Adegoke, A. Beltran-Przekurat, C. Hiemstra, J. Lin, U. Nair, D. Niyogi, and T. Nobis (2007b), An overview of regional land-use and land-cover impacts on rainfall, *Tellus B*, *59*(3), 587–601.

Pielke, R. A., A. Pitman, D. Niyogi, R. Mahmood, C. McAlpine, F. Hossain, K. K. Goldewijk, U. Nair, R. Betts, and S. Fall (2011), Land use/land cover changes and climate: Modeling analysis and observational evidence, *Wiley Interdiscip. Rev. Clim. Change*, *2*(6), 828–850.

Puma, M., and B. Cook (2010), Effects of irrigation on global climate during the 20th century, *J. Geophys. Res.*, *115*, D16120, doi:10.1029/2010JD014122.

Rigo, G., E. Parlow, and D. Oesch (2006), Validation of satellite observed thermal emission with in situ measurements over an urban surface, *Remote Sens. Environ.*, *104*, 201–10.

Sacks, W. J., B. I. Cook, N. Buenning, S. Levis, and J. H. Helkowski (2009), Effects of global irrigation on the near-surface climate, *Clim. Dyn.*, *33*(2–3), 159–175.

Sampaio, G., C. Nobre, M. H. Costa, P. Satyamurty, B. S. Soares-Filho, and M. Cardoso (2007), Regional climate change over eastern Amazonia caused by pasture and soybean cropland expansion, *Geophys. Res. Lett.*, *34*, L17709, doi:10.1029/2007GL030612.

Shi, W., F. Tao, and J. Liu (2014), Regional temperature change over the Huang-Huai-Hai Plain of China: The roles of irrigation versus urbanization, *Int. J. Climatol.*, *34*(4), 1181–1195.

Siebert, S., V. Henrich, K. Frenken, and J. Burke (2013), Update of the digital global map of irrigation areas to version 5. Rheinische Friedrich-WilhelmsUniversität, Bonn, Germany and FAO, Rome, Italy.

Tachikawa, T., M. Hato, M. Kaku, and A. Iwasaki (2011), Characteristics of ASTER GDEM version 2, paper presented at Geoscience and Remote Sensing Symposium (IGARSS), 2011 IEEE International, IEEE.

Vitousek, P. M., H. A. Mooney, J. Lubchenco, and J. M. Melillo (1997), Human domination of Earth's ecosystems, *Science*, *277*(5325), 494–499.

Voogt, J. A., and T. R. Oke (2003), Thermal remote sensing of urban climates, *Remote Sens. Environ.*, *86*(3), 370–384.

Wan, Z. (2008), New refinements and validation of the MODIS land-surface temperature/emissivity products, *Remote Sens. Environ.*, *112*(1), 59–74.

Wan, Z. (2014), New refinements and validation of the collection-6 MODIS land-surface temperature/emissivity product, *Remote Sens. Environ.*, *140*, 36–45.

Wan, Z., and J. Dozier (1996), A generalized split-window algorithm for retrieving land-surface temperature from space, *IEEE Trans. Geosci. Remote Sens.*, *34*(4), 892–905.

Woldemichael, A. T., F. Hossain, and R. Pielke Sr. (2014), Impacts of postdam land use/land cover changes on modification of extreme precipitation in contrasting hydroclimate and terrain features, *J. Hydrometeorol.*, *15*(2), 777–800.

Wu, S., Y. Yin, D. Zheng, and Q. Yang (2005), Aridity/humidity status of land surface in China during the last three decades, *Sci. China Ser. D Earth Sci.*, *48*(9), 1510–1518.

Xiao, X., S. Boles, S. Frolking, C. Li, J. Y. Babu, W. Salas, and B. Moore (2006), Mapping paddy rice agriculture in South and Southeast Asia using multi-temporal MODIS images, *Remote Sens. Environ.*, *100*(1), 95–113.

Zhang, P., M. L. Imhoff, R. E. Wolfe, and L. Bounoua (2010), Characterizing urban heat islands of global settlements using MODIS and nighttime lights products, *Can. J. Remote Sens.*, *36*(3), 185–196.

Zhao, L., X. Lee, R. B. Smith, and K. Oleson (2014), Strong contributions of local background climate to urban heat islands, *Nature*, *511*(7508), 216–219.

Zhou, D., S. Zhao, S. Liu, and L. Zhang (2014a), Spatiotemporal trends of terrestrial vegetation activity along the urban development intensity gradient in China's 32 major cities, *Sci. Total Environ.*, *488*, 136–145.

Zhou, D., S. Zhao, S. Liu, L. Zhang, and C. Zhu (2014b), Surface urban heat island in China's 32 major cities: Spatial patterns and drivers, *Remote Sens. Environ.*, *152*, 51–61.

Zhou, D., S. Zhao, L. Zhang, G. Sun, and Y. Liu (2015), The footprint of urban heat island effect in China, *Sci. Rep.*, *5*.

Zhou, D., L. Zhang, L. Hao, G. Sun, Y. Liu, and C. Zhu (2016a), Spatiotemporal trends of urban heat island effect along the urban development intensity gradient in China, *Sci. Total Environ.*, *544*, 617–626.

Zhou, D., S. Zhao, L. Zhang, and S. Liu (2016b), Remotely sensed assessment of urbanization effects on vegetation phenology in China's 32 major cities, *Remote Sens. Environ.*, *176*, 272–281.

Zhou, L., R. E. Dickinson, Y. Tian, J. Fang, Q. Li, R. K. Kaufmann, C. J. Tucker, and R. B. Myneni (2004), Evidence for a significant urbanization effect on climate in China, *Proc. Natl. Acad. Sci. U. S. A.*, *101*(26), 9540–9544.